PHYSICAL REVIEW D

PARTICLES AND FIELDS

THIRD SERIES, VOLUME 30, NUMBER 10 15 NOVEMBER 1984

Tapered cylinder antenna for gravitational radiation: Design and tests of a prototype

Munawar Karim

Department of Physics and Astronomy, University of Rochester, Rochester, New York 14627
and Department of Physics, St. John Fisher College, Rochester, New York 14618

(Received 4 June 1984)

In an effort to increase the coupling between a gravitational radiation antenna and transducer the ends of a small cylindrical prototype antenna were tapered to magnify the end motion by a factor of 20. Flexural rigidity was maintained by tapering the inside of the cylindrical antenna. The algorithm used to calculate the taper is described. Experimental tests on the prototype antenna confirm the correctness of the algorithm. Results thus obtained indicate that much larger amplification is possible in full-scale antennas. The consequent decrease in the noise temperature is shown to be sufficient to improve the sensitivity of a resonant-mass gravitational radiation detector by at least an order of magnitude. As a result of the stronger coupling, the bandwidth is also increased.

I. INTRODUCTION

Although gravitational radiation antennas may have a variety of shapes, the uniform cylinder resonant-mass type is most commonly used. Advantages of simplicity and of a high filling factor inside conventional cryostats have made the latter the most popular choice so far.

Much has been written on the subject of coupling the end face of cylindrical antennas to transducers.[1] The ratio of the energy transferred to the transducer to the energy in the antenna, usually denoted by β, is a measure of the coupling between antenna and transducer. For nonresonant transducers, β is usually between 10^{-6} to 10^{-4}. Increasing β beyond 10^{-3} does not appear to be feasible with present nonresonant transducers because of physical limitations such as critical fields in superconductors or maximum possible static electric fields.

One reason why the efficiency of energy transfer from a uniform cylinder antenna to a transducer is so small is the large impedance mismatch at the interface. The impedance mismatch can be reduced by using either a mechanically or electrically resonant transducer[2] resulting in an improvement in β but possibly at the expense of degraded time resolution for impulse detection.

Another route towards increasing β is to introduce a tapered section at the ends of a uniform cylinder. For nonresonant transducers, this new shape offers the possibility of values of $\beta > 10^{-3}$ as well as an increase in the bandwidth. In this paper we will discuss results of experiments with a tapered cylinder as well as the feasibility of translating these results to a full-size antenna.

Possible shapes for tapered cylinders have been calculated in three papers.[3–5] In a brief report, Aplin has described a variant of a dumbbell antenna with exponential horns. Gowdy has shown that a cylindrical antenna with a Gaussian taper may be used to discriminate against unwanted excitations because only the fundamental longitudinal mode couples to gravitational waves. Bonazzola and Chevreton's study of an approximately conical antenna suggests that it is four times more sensitive than a uniform cylinder because the end-face oscillation is amplified by 2. The last two papers are of a theoretical nature: how the ends of the tapered cylinders are to be coupled to transducers or questions about the effect of noise introduced by amplifiers have not been emphasized, so the conclusions arrived at are at best incomplete.

II. METHOD FOR OBTAINING TAPER

The basic idea is to amplify the motion of the end faces of a cylinder (assumed to be right circular) by altering the mass/length (linear mass density) from center to outer end of a cylinder.

Assuming azimuthal symmetry and length $\gg$ radius, the differential equation for longitudinal displacement amplitude of longitudinal waves in a steadily vibrating homogeneous cylinder of nonuniform cross section is[6]

$$U''+U'\frac{d}{dX}\ln A(X)+\Omega^2 U=0\ , \tag{1}$$

where $X=x/L$, $U=u/L$, and $\Omega=2\pi L/\lambda$. L is the length of the tapered section. λ is the wavelength of longitudinal waves in a thin uniform cylinder, x is the coordinate, u is the longitudinal displacement from equilibrium at X, and $A(X)$ is the ratio of the area of cross section of the cylinder at X with respect to the area at $X=0$.

Primes denote derivatives with respect to X. This equation neglects second-order terms as well as damping.

Given an analytic function for $A(X)$ (such as exponential, catenoidal, conical, etc.), one can solve for $U(X)$. The amplitude of end motion can be obtained and compared to that of a cylinder of uniform cross section. Several examples have been reviewed.[7,8] It is immediately apparent that, for the limited number of analytical functions available for $A(X)$, magnification beyond about 10 is not practical because the thinnest section is virtually a whisker. Because of poor flexural rigidity, the ability to machine such shapes, not to speak of trying to couple a whisker to a transducer, becomes questionable.

One is faced with the following problem: Find a curve for $A(X)$ that will give the maximum magnification within practical limits with sufficient flexural rigidity. At the same time the end face should be of a shape to allow easy coupling to a transducer.

We proceed by rewriting Eq. (1) as

$$\frac{d}{dX}\ln A(X)=-\frac{U''+\Omega^2U}{U'}\,. \tag{2}$$

If the normalized wave function U is expressed as a Fourier series, then for a given set of boundary conditions (which includes the magnification) we may obtain the coefficients of the series. For a given magnification, there exists a curve for $A(X)$ which is obtained by repeatedly integrating Eq. (2).

The integral equation method has one signal advantage: one obtains a taper $A(X)$ for a given magnification[6] a result not obtainable by conventional methods.

For simplicity we choose to confine the tapered section to $\frac{1}{8}$ of the wavelength (the cylinder length is $\lambda/2$ for the $1L$ mode, so $\Omega=\pi/4$) on either end of a cylinder which is otherwise of uniform cross section. (In general, the length of the tapered section is a free parameter.)

For the first longitudinal mode we choose a composite wave function which is sinusoidal with a node at the center of the cylinder ($X=-1$) and an amplitude U_0 at $X=0$, where the cylinder cross section starts to taper. Within the tapered section the wave function is the sum of a Fourier series that is smoothly matched to the amplitude U_0 at $X=0$ and attains a magnified amplitude MU_0 at the free end $X=+1$. The wave function is antisymmetric about $X=-1$.

The composite wave function is

$$\frac{U}{U_0}=\cot\Omega\,\sin\Omega X+\cos\Omega X \tag{3}$$

in the region $-1\le X\le 0$ and

$$\frac{U}{U_0}=\sum_{n=0}^{N}\alpha_n\sin nX\frac{\pi}{2}+\sum_{n=0}^{N}\beta_n\cos nX\pi \tag{4}$$

in the region $0\le X\le +1$, where α_n and β_n are unknown Fourier coefficients.

We specify the conditions to be satisfied at the transition point ($X=0$) and at the free end ($X=1$). The magnification M is now the sole input parameter. [Compare this to conventional methods where $A(X)$ is the input parameter and M is an *output* parameter.]

TABLE I. Boundary conditions for the wave function at $X=0$ and $X=1$.

$X=0$	$X=1$
$U=U_0$	$U=MU_0$
$U'=U_0\Omega\cot\Omega$	$U'=0$
$U''=-\Omega^2U_0$	$U''=-M\Omega^2U_0$
$U'''=-\Omega^3U_0\cot\Omega$	$U'''=0$

Thus, at $X=0$ and $X=1$ we demand that the wave function and its derivatives acquire the values shown in Table I. These eight conditions ensure that Eq. (2) is finite everywhere. Furthermore, the gradient of the lateral surface is made to vanish both at $X=0$ and $X=1$. This gives the most economical taper for a given ratio of maximum to minimum cross-sectional areas.[6]

Since there are eight boundary conditions we choose $N=3$ which gives us eight coefficients and as many equations. With the Fourier coefficients determined by imposing the boundary conditions, one gets an expression which may be integrated numerically (or even analytically) from a lower limit $X=0$ to an upper limit X incremented by small intervals to give $\ln A(X)$ and thus $A(X)$:

$$\ln A(X)=\ln\left[\frac{a(X)}{a(0)}\right]=-\int_0^X\frac{U''+\Omega^2U}{U'}dX\,. \tag{5}$$

The required flexural rigidity obtains, if we use an inverse taper, where the taper is on the inside of a hollow cylinder. For example, the inverse taper radius $R(X)$ for a cylinder of outer radius R_0 is obtained from the expression

$$R(X)=R_0[1-a(X)/a(0)]^{1/2}\,. \tag{6}$$

Carrying out the computation outlined above for a cylinder of radius 1.91 cm and tapered section of length $L=5.08$ cm (total length 20.32 cm), and choosing as input parameter a magnification factor $M=20$, we get values of $R(X)$ vs X as plotted in Fig. 1. The wall thickness is 0.16 mm at the point of minimum cross section. Values of α_n and β_n are listed.

We note that the lip at the end of the cylinder may be readily coupled to a transducer. A pair of light, stiff aluminum disks (mass$\approx$2 gram) were secured to the ends of the cylinder by means of brass screws. The stiffness of the disk is chosen to push its lowest resonant frequency above the IL mode of the cylinder. The mass is kept to a minimum to minimize loading effects. (In principle, the

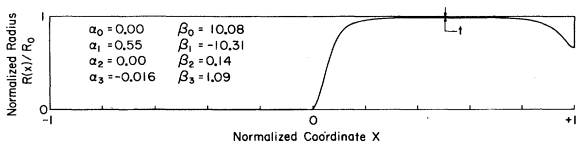

FIG. 1. Section of antenna showing the inverse taper in one quadrant. Coordinate extends from center of antenna at $X=-1$ to the free end at $X=+1$. Tapered section is between $X=0$ and $X=+1$. Radius of inverse taper is shown as $R(X)$. Fourier coefficients α_n and β_n are also listed.

shape of the lip may be modified to accommodate the extra mass of the disk.) Once the disks are in place, the ends of the cylinder look like a uniform cylinder in so far as coupling to a transducer is concerned. For example, the disks may be made to superconduct by covering them with a lead film to couple the cylinder to a Rochester-type inductive noncontacting transducer. Or a light resonant vane may be machined into a disk for a back-action-evading transducer whose principles were described in an earlier paper.[9] For the latter case which uses a resonant transducer, only one end of the cylinder needs to be tapered.

III. EXPERIMENTAL TESTS

The ends of a cylinder of aluminum alloy 5052 F (sound velocity = 5095 m/sec at room temperature[10]), 20.32 cm long and 3.81 cm in diameter were machined to the taper shown in Fig. 1. The $1L$ mode is expected to have a frequency of 12 537 Hz.

In order to study its eigenmodes the cylinder was mounted on a four-point support resting on a platform which could be moved on a horizontal plane by a pair of micrometers. The disks were removed. The cylinder was driven by impressing signals from a frequency synthesizer on a small piezoelectric strain gauge glued near the center of the cylinder.

Cylinder vibration amplitudes were measured using a displacement sensor made from a stereo phonograph needle. With this device it is possible to measure both radial and axial displacements (as well as the relative phases) to an accuracy of better than $10^{-9}m_{\text{rms}}$.

The two output channels from the stereo cartridge were fed to a lock-in amplifier using the driving frequency as reference. Using the pair of micrometers to position the needle, radial and axial oscillation amplitudes were measured at several points along the length of the cylinder.

A few of the wave functions measured in this manner are shown in Fig. 2. Important modes identified thus are the flexural and longitudinal modes listed in Table II.

Because the incident gravitational radiation couples to the $1L$ mode, we will discuss the properties of this mode in detail. A curve is drawn through the points for the $1L$ mode in Fig. 2 using calculated values of α_n and β_n from Fig. 1.

There are a few noticeable deviations from the predicted behavior. There is a relative shift in the abscissa of calculated and measured wave functions. In fact, the fractional shift in the abscissa is just equal to the 11% reduction in the measured frequency from the predicted value.

The measured wave function peaks at $X=0.9$ instead of $X=1.0$ and shows a noticeable droop near the edge at

TABLE II. Eigenmodes and frequencies of the tapered cylinder. F—flexural, L—longitudinal.

$1F$(@ 3 818 & 3 827 Hz)	$1L$(@ 11 300 Hz)
$2F$(@ 4 818 & 4 832 Hz)	$2L$(@ 12 550 Hz)
$3F$(@ 11 812 & 12 069 Hz)	$3L$(@ 23 312 Hz)

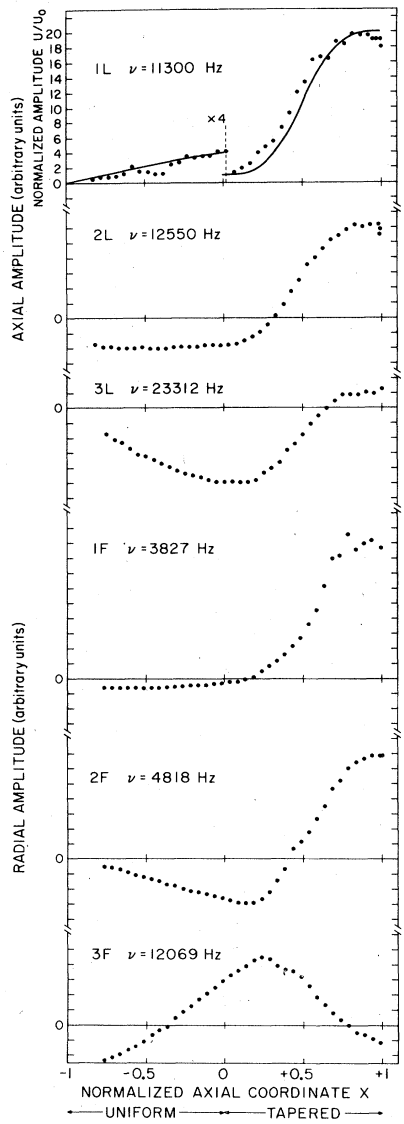

FIG. 2. Measured eigenfunctions of tapered cylinder. Labels L and F denote longitudinal and flexural modes. The abscissa common to all graphs is the normalized axial coordinate X. Ordinates measure axial amplitudes for longitudinal modes and amplitudes perpendicular to the axis for flexural modes. Ordinate for the $1L$ mode is in normalized units U/U_0; calculated wave function is shown as a line through the points.

$X=1.0$, indicating a nonzero strain at the free end. These discrepancies may be explained by the combined effect of a small force exerted by the sensor on the end of the cylinder, i.e., the cylinder is not truly "free" at the end, as well as minor deviations from the calculated taper due to imperfect machining.

In a real antenna the end facing the transducer will not be free either but will see an impedance corresponding to the loading effect of the transducer and preamplifier. This must be taken into account in designing the required taper for real antennas. The method to be used is described by Eisner.[11]

The magnification is 19.0 ± 0.5 as compared to the predicted value 20. Clearly, the end motion of a tapered cylinder under longitudinal excitation is amplified in a manner consistent with the results of the algorithm.

We should clarify that magnification here means the ratio of amplitudes between the ends of the tapered section. Compared to the end motion of a uniform cylinder, the tapered cylinder vibrates with an amplitude enhanced by $M2^{-1/2}$.

IV. EXTENSION OF RESULTS TO REAL ANTENNAS

It is possible to scale up the results we have obtained so far for a prototype tapered cylinder antenna. From calculations of $A(X)$ for different values of M we find that within the linear approximation the magnification varies inversely as the minimum wall thickness t. In Fig. 3 we show the magnification versus minimum wall thickness for cylinders of various radii (R_0). The straight lines follow the equation

$$M \approx \frac{1}{6}\frac{R_0}{t} . \tag{7}$$

For the University of Rochester gravitational radiation antenna which is an aluminum cylinder of radius 15.24 cm, a magnification of 32 is possible for a tapered section with minimum wall thickness of $t=0.8$ mm. For a cylinder of radius 50 cm and $t=0.8$ mm, the magnification exceeds 100.

It is apparent that an amplifying tapered section is identical to a step-down transformer for stepping down the force and stepping up the velocity of displacement.

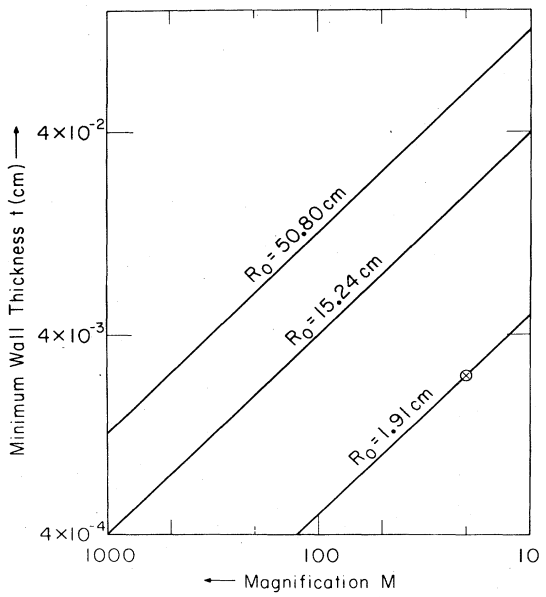

FIG. 3. This log-log plot shows calculated values of the magnification M vs minimum wall thickness t for tapered antennas of outer radius R_0. Circled point corresponds to prototype antenna.

Thus, both the mass and spring constant of an equivalent simple harmonic oscillator are reduced by $M^2/2$ leaving the frequency of the $1L$ mode unchanged. The impedance seen by the transducer at the $1L$ resonance is decreased by $M^2/2$ and hence also the degree of mismatch between transducer and cylinder relative to a cylinder of uniform cross section. Energy transfer is more efficient and β is increased by $M^2/2$ and so is the optimum bandwidth by the same factor (Ref. 12, Appendix C).

We note that when compared to a single mechanically resonant diaphragm transducer, the tapered section just described appears to be analogous to a continuum of an infinite number of discrete diaphragms whose mass distribution follows the curve for $A(X)$. Mechanically resonant diaphragms have associated with them a beat period of energy transfer between the cylinder and diaphragm which sets a lower limit on the integration time (causing the degraded time resolution mentioned previously) over and above that due other factors such as Brownian motion, back action, and amplifier noise. In the continuous case the beat period is eliminated so that the optimum integration time is determined solely by the last three factors. The consequent increase in the bandwidth is important when searching for coincidences between excitations in widely separated antennas.

There are some limitations, however. If we keep reducing the fractional length of the tapered section, then at some point the equation of motion becomes nonlinear, i.e., the area of cross section is no longer "smoothly varying." Furthermore, in order to achieve high magnification, the ability to machine very thin wall sections is of paramount importance.

Another requirement is a large mechanical quality factor Q at low temperatures. The parent sample of 5052 aluminum alloy had a $Q=2.4\times10^7$ at 4°K.[10] The $1L$ mode of the tapered cylinder had a room temperature Q of about 10^4. We are studying the low-temperature properties and other aspects of the tapered cylinder. Complete results will be reported in a future publication.

V. MINIMUM DETECTABLE FLUX

It has been shown[13] that the energy flux density of the minimum noise-equivalent impulse of gravitational radiation is

$$\Phi_n = kT_n/\Sigma , \tag{8}$$

where T_n is the minimum noise temperature of the antenna and amplifier, Σ is the gravitational cross section of the antenna, and k is the Boltzmann constant. Φ_n improves as T_n is lowered and/or Σ is increased.

If a uniform cylinder and a tapered cylinder have identical frequencies for the first longitudinal mode, as is the case here, it can be shown that the gravitational cross section of the latter is approximately that of a uniform cylinder whose length is the same as the length of the uniform section of the tapered cylinder. For the double-sided tapered cylinder described here, the uniform section is half the total length, hence the gravitational cross section is reduced by $(\frac{1}{2})^3$ when compared to a uniform cylinder.

For a similar cylinder with a single-sided taper, the reduction factor is $(\frac{3}{4})^3$. If the tapered section is $\frac{1}{12}$ the total length, then Σ is reduced by $(\frac{11}{12})^3$.

Under optimum filtering conditions and negligible electrical losses the minimum noise temperature may be written as[12]

$$T_n = 2T_A \left[(1+\gamma^2) \left[1+\frac{2\alpha}{\gamma\beta Q} \right] \right]^{1/2} \tag{9}$$

in terms of $\alpha \equiv T/T_A$ the physical temperature to amplifier noise temperature ratio and $\gamma \equiv Z_A/Z_T$ the amplifier noise impedance to transducer impedance ratio. Mechanical losses in the antenna are represented by Q. Noise temperature is minimum when both γ^2 and $2\alpha/\gamma\beta Q \to 1$. Matching of transducer and antenna occurs when $2\alpha/\gamma\beta Q \to 1$. Other parameters being fixed, T_n is inversely proportional to $\beta^{1/2}$ until transducer and antenna are optimally matched.

The coupling factor β is directly proportional to the square of the magnification factor M, so that β for the tapered cylinder is $(20\times 2^{-1/2})^2 = 200$ times that of a uniform cylinder. The bandwidth is increased by a factor of 200 also. Furthermore, in spite of the smaller Σ, Φ_n for the prototype tapered cylinder is about half that of a uniform cylinder of the same overall length which is a net improvement in the sensitivity.

If we reduce the length of the tapered section to $(2\times\frac{1}{12})$ of the total length (this is still in the linear regime), then for a double-sided tapered cylinder a net improvement in Φ_n obtains when $M > 3$. For a single-sided tapered cylinder the corresponding figure is $M > 2$. In the previous section we have indicated that much larger values of M are possible.

It is clear that by tapering a cylinder in the manner described above, antenna and transducer can be optimally matched because β may be increased by 10^2 to 10^4, with a corresponding decrease in Φ_n by a factor of 10 to 100 in real antennas. These conclusions are valid as long as the detector sensitivity is not limited by amplifier noise. We note that the amplifier limit is reached more easily using a tapered cylinder. On the other hand, if the detector sensitivity is already amplifier limited, then a larger bandwidth is gained by using a tapered cylinder.

Finally we note that when antenna and transducer are optimally matched, the resonant frequency is determined by the total impedance of antenna and transducer.[1] Because of the extraordinary sensitivity of the frequency of a tapered cylinder antenna to loading effects of the transducer, it is possible to achieve a degree of tunability by varying the coupling fields and hence the impedance of the transducer.

ACKNOWLEDGMENTS

My interest in tapered cylinder antennas for gravitational radiation stems from earlier work by Alan Hoffman. The displacement sensor used to measure wave functions was designed and built by Mark Bocko. I am grateful to him for allowing me to use it. Discussions during the course of this work, as well as critical readings of the manuscript by my colleagues M. Bocko, R. Q. Gram, W. W. Johnson, B. Muhlfelder, and L. Narici, resulted in several useful suggestions which improved the contents of this paper. Close agreement between measured and predicted results testifies to the precision machining skills of P. Borelli. I acknowledge with gratitude all of their contributions. This work was supported by the National Science Foundation.

[1] G. V. Pallotino and A. Pizzella, Nuovo Cimento **4C**, 237 (1981).

[2] L. Narici, J. Appl. Phys. **53**, 3941 (1982); H. J. Paik, *ibid.* **47**, 1168 (1976).

[3] P. S. Aplin, in *Abstracts of Contributed Papers, 8th International Conference on General Relativity and Gravitation* (University of Waterloo, Ontario, 1977), p. 360.

[4] R. H. Gowdy, Phys. Rev. D **15**, 969 (1977).

[5] S. Bonazolla and M. Chevreton, Phys. Rev. D **8**, 359 (1973).

[6] E. Eisner, J. Acoust. Soc. Am. **35**, 1367 (1963).

[7] J. C. Snowdon, *Vibration and Shock in Damped Mechanical Systems* (Wiley, New York, 1968).

[8] A. W. Hoffman, G-Lab Tech. Memo 183, 1977, University of Rochester (unpublished).

[9] M. Bocko, L. Narici, D. H. Douglass, and W. W. Johnson, Phys. Lett. **97A**, 259 (1983).

[10] D. H. Douglass, G-Lab Tech. Memo 218, 1979, University of Rochester (unpublished).

[11] E. Eisner, J. Acoust. Soc. Am. **41**, 1126 (1967).

[12] M. Bocko, M. W. Cromar, D. H. Douglass, R. Q. Gram, W. W. Johnson, M. Karim, C. C. Lam, D. Macaluso, J. R. Marsden, B. Muhlfelder, L. Narici, and M. Zucker, J. Phys. E **17**, 694 (1984).

[13] C. W. Misney, K. S. Thorne, and J. A. Wheeler, *Gravitation* (Freeman, San Francisco, 1973).